DESIGN STUDY FOR A 200 GHZ GYROTRON

R.J. Temkin and S.M. Wolfe

Plasma Fusion Center
Research Report RR-78-9

March 9, 1978

Design Study for a 200 GHz Gyrotron

by

R.J. Temkin and S.M. Wolfe

Francis Bitter National Magnet Laboratory*

Massachusetts Institute of Technology

Cambridge, Ma. 02139

Plasma Fusion Center Research Report RR-78-9

*Supported by NSF

ABSTRACT

A complete design of a 200 GHz gyrotron is presented using a combination of analytic expressions and numerical results primarily derived from the Soviet literature. The design study is divided into two parts: Part I, which outlines general design principles, and Part II, which gives specific parameters for a 10kW, 200 GHz gyrotron. In Part I, the major topics treated are gyrotron cavity design, gyrotron gun design, starting current, efficiency, constraints on parameter selection and wavelength scaling of gyrotron parameters. Most of the theoretical expressions used are taken from a series of Soviet publications on the gyrotron. However, some new results have been obtained, including some new expressions for the wavelength scaling of gyrotron parameters. The design criteria have been applied to predicting the efficiency of gyrotrons operating at the fundamental (ω_c) or second harmonic ($2\omega_c$) frequency. In the wavelength range 0.5 to 5.0 mm, fundamental emission is found to be significantly more efficient than second harmonic emission. Agreement with the experimental and theoretical efficiency results of Zaytsev _et al_. is reasonably good, indicating that the design procedure is accurate. Prior to constructing a device, however, more precise calculations of several parameters, such as beam velocity spread and cavity diffractive Q, is warranted in order to achieve optimum device performance. In Part II, a complete set of design parameters is derived for a 10kW, 200 GHz gyrotron. The mirror ratio is chosen to be 25 and the overall efficiency is predicted to be 32%.

DESIGN STUDY FOR A
200 GHZ GYROTRON

Part I

R.J. TEMKIN, S.M. WOLFE

Francis Bitter National Magnet Laboratory
Massachusetts Institute of Technology
Cambridge, Massachusetts 02139 USA

March 9, 1978

GYROTRON DESIGN - GENERAL PRINCIPLES

A. Introduction

B. Gyrotron Cavity

- i) Cavity mode
- ii) Ohmic Q, Q_{OM}
- iii) Diffractive Q, Q_D
- iv) Oscillation Frequency, ω
- v) Magnetic field in Cavity Region, B_o

C. Gyrotron Gun

- i) Definitions
- ii) Correlation of Gun and Cavity Parameters
- iii) Velocity Spread
  - a) Space charge at the cathode.
  - b) Thermal velocity of electrons.
  - c) Surface roughness of the cathode.

D. Starting Current and Efficiency

- i) Starting Current
- ii) Multimode Oscillation
- iii) Efficiency

E. Design Considerations

- i) Cavity Length
- ii) Mirror Ratio
  - a) Parameter Scaling with α.
  - b) Constraints on the gun design.

F. Wavelength Scaling of Gyrotron Parameters

i) General Wavelength Scaling

ii) Efficiency vs. Wavelength

G. References

GYROTRON DESIGN

A. Introduction

Soviet workers have outlined many of the design principles for their gyrotrons in a series of publications. Those principles may be summarized by a relatively simple analytic theory which is very useful for preliminary gyrotron design and is applied in the present design study. It should be recognized that many of the final design parameters must be obtained from more accurate, computer calculations in order to achieve the highest possible device efficiency. The analytic theories used here do serve to define the approximate value of many parameters and so are of great use in preliminary designs.

The gyrotron design may be divided into two major subsystems, the electron gun and the cavity, which are physically distinct units. However, the design of these two subsystems is not independent. All of the parameters for the design of a gyrotron are evaluated by methods described below. Some parameters, such as the cavity length, require more detailed computer calculations if a highly optimized device is desired. As a check of the present design procedures, the same methods have been applied to evaluate several experimental Soviet gyrotrons. In particular, we have rederived the scaling laws for gyrotron parameters vs. wavelength presented by Zaytsev et al. We have also calculated the theoretical efficiency of Zaytsev's gyrotrons and obtain good agreement with the published theoretical and experimental efficiencies. Hence, the analytic approach to gyrotron design is reasonably accurate and has the advantage of great simplicity. In the present study, only operation at the cyclotron fundamental, $\omega \sim \omega_c$, is considered.

B. Gyrotron Cavity

i) Cavity Mode

A typical gyrotron cavity is depicted in Fig. 1. The cavity shown is similar to those described and analyzed in the Soviet literature. The cavity shown has no taper, although tapering may improve efficiency and may be included in later designs. The cavity resonance conditions are taken as those for a right circular cylinder. The mode will be a TE_{mpq} mode. The transverse index is X_{mp} where X_{mp} is the p^{th} zero of $J_m'(y) = 0$. We assume that $L/\lambda >> 1$, where λ is the wavelength. This assumption is justified below. Then,

$$D_o = 2R_o = \frac{X_{mp}}{\pi} \lambda \tag{1}$$

In order to further simplify the present discussion, we immediately specialize to the case:

$$m = 0, \; q = 1, \; p \text{ arbitrary} \tag{2}$$

The choice $m = 0$ appears to be the optimum for low mode operation at $\omega = \omega_c$. The extension to $m \neq 0$ will be obvious from the treatment given here. The choice $q = 1$ is important for maintaining single mode operation and achieving high efficiency.

The beam radius, R_e, must be matched to a maximum in the transverse RF field distribution. This requires:

$$J_1 \, (X_{op} R_e / R_o) = \text{maximum}$$

or $$J_1' \, (X_{op} R_e / R_o) = 0$$

or $$X_{op} \, R_e / R_o = X_{11}, \, X_{12}, \, X_{13}, \, \cdots \text{ or } X_{1p}$$

Let the beam coincide with the r^{th} maximum. Then

$$R_e = \frac{X_{1r}}{X_{op}} R_o \text{ , } 1 \leq r \leq p \tag{3}$$

ii) OHMIC Q, Q_{OM}

The theoretical ohmic Q, Q_{OM} is given, for a TE_{opl} mode, by

$$Q_{OM} = \frac{R_o}{\delta} \frac{X_{op}^2 + \left(\frac{\pi}{2}\right)^2 r^2}{X_{op}^2 + \left(\frac{\pi}{2}\right)^2 r^3} \tag{4}$$

where $r = D_o/L$ and δ is the skin depth. For $L/\lambda >> 1$, Q_{OM} is given to high accuracy by:

$$Q_{OM} = R_o/\delta \tag{5}$$

For a copper cavity at $\lambda = 2$ mm, $\delta = 1.7 \times 10^{-5}$cm. It is important to allow for a somewhat degraded Q_{OM} due to surface imperfections, particularly at short wavelengths. For example, it may be better to assume

$$Q_{OM} = \Lambda R_o/\delta \tag{6}$$

$$\Lambda \approx 0.5 - 0.8$$

iii) Diffractive Q, Q_D

The diffractive Q of the resonator is given by

$$Q_D = 4\pi \frac{L^2}{\lambda^2} \frac{1}{1 - |R_1 R_2|} \tag{7}$$

where R_1, R_2 are the electric field reflection amplitude coefficients at the two ends of the cavity. The mimimum cavity Q is given by:

$$Q_{MIN} = 4\pi L^2/\lambda^2 \tag{8}$$

and we may redefine Q_D as:

$$Q_D = K\ Q_{MIN} \tag{9}$$

In general, the parameter K varies with cavity shape, mode, length and diameter. For the cavity shown in Fig. 1, K is not a strong function of cavity mode and a rough value of $K \approx 3$ is obtained. Hence $Q_D \approx 3\ Q_{MIN}$. The total cavity Q is given by:

$$\frac{1}{Q} = \frac{1}{Q_D} + \frac{1}{Q_{OM}} \tag{10}$$

and it is important to have $Q_D << Q_{OM}$ to achieve high efficiency.

iv) Oscillation Frequency, ω

When $(X_{op}/R_o) >> (\pi/L)$, then

$$\omega = \omega_{cr}\ [1 + \delta_1(\lambda_{cr}/L)^2] \tag{11}$$

where

$$\omega_{cr} = 2\pi\ c/\lambda_{cr} = 2\ X_{op}C/D_o \tag{12}$$

For a right circular cylinder cavity, δ_1 is given by

$$\delta_1 = 0.125 \tag{13}$$

and is independent of cavity dimensions. For other cavity shapes, δ_1 is a function of cavity dimensions and must be obtained from detailed calculations. In the present study, with $L/\lambda >> 1$, the term $\delta_1(\lambda_{cr}/L)^2$ is much less than one and can be ignored with an error of less than about two parts in 10^3. In that case, $\lambda \approx \lambda_{cr}$ and the cavity is very close to the cutoff condition. Also, Eq. (11) reduces to Eq. (1) in this limit. Eq. (1) was assumed earlier in order to clarify the discussion of the cavity dimensions.

v) Magnetic field in the cavity region, B_o

The maximum device gain occurs when

$$\omega - \omega_c = k_{\parallel} v_{\parallel} \tag{14}$$

Here,
$$\omega_c = \frac{eB_o}{\gamma m_o C} \tag{15}$$

and $k_{\parallel} = q\pi/L = \pi/L$. γ is the relativistic increase in rest electron mass, m_o. Since $k_{\parallel}$ and ω are obtained from the cavity design and $v_{\parallel}$ from the gun design, Eq. (14) yields B_o. The value of $k_{\parallel}v_{\parallel}$ is relatively small so as to minimize the importance of the Doppler effect in maintaining the resonance condition as the electrons lose energy in the cavity. That is,

$$\frac{k_{\parallel} v_{\parallel}}{\omega} = \frac{1}{2}\, \beta_{\parallel} \frac{\lambda}{L} << 1$$

The electron gyroradius, r_g, is given by:

$$r_g = \frac{v_{\perp}}{\omega_c} = \frac{c\beta_{\perp}}{\omega_c} \approx \frac{c\beta_{\perp}}{\omega} = \frac{\beta_{\perp}\lambda}{2\pi} \tag{16}$$

The ratio of r_g to the beam radius R_e is:

$$\frac{r_g}{R_e} \approx \frac{\beta_{\perp}\lambda}{2\pi} \frac{1}{R_o(X_1/X_{op})} = \frac{\beta_{\perp}}{X_{1r}}, \quad 1 \leq r \leq p$$

Hence $r_g << R_e$ and the electron beam is in the form of a hollow cylinder.

C. Gyrotron Gun

i) Definitions

A typical gyrotron gun is illustrated schematically in Fig. 2. The fundamental parameters of the gun may be defined as follows:

B_k = Magnetic field in the gun region.

B_o = Magnetic field in the cavity region

$2R_k$ = Diameter of emitting strip

ℓ_k = width of emitting strip

d = cathode to first anode spacing

V_1 = First anode to cathode voltage

ϕ = Angle between cathode surface and $\bar{B}$

The electron beam must also be defined using the following parameters:

$v_\parallel, v_\perp$ = velocity components in cavity region

$v_{\parallel k}, v_{\perp k}$ = velocity components near the cathode

U = total energy of each electron at the cavity

I = Electron current (in statamps unless otherwise indicated)

From the above definitions, a number of additional parameters may be defined or calculated. Assume that the electrons have energy U in the cavity region, where U is the potential difference between cathode and ground. Then, γ and $\beta = v/c$ are given by:

$$\gamma = \frac{1}{\sqrt{1 - \beta^2}} = 1 + \frac{U}{511 \text{ keV}} \tag{17}$$

The mirror ratio, α, is defined by

$$\alpha = B_o/B_k \tag{18}$$

The perpendicular electric field near the cathode is given by

$$E_{\perp k} = \frac{V_1}{R_k} \frac{1}{\ell n\left(\frac{R_k + d}{R_k}\right)} \approx \frac{V_1}{d} \text{ for } d << R_k \tag{19}$$

The electrons coming from the emitting strip travel a distance h along the magnetic field during the time required to make one cyclotron orbit, where

$$h = 2\pi^2 \phi_k r_{\perp k} \tag{20}$$

The emitter strip area A is given by,

$$A = 2\pi R_k \ell_k$$

and the emitter current density, J_k, is

$$J_k = I/2\pi R_k \ell_k \tag{21}$$

The initial height to which an electron rises above the emitter strip is $2r_{\perp k}$ where:

$$r_{\perp k} = \frac{v_{\perp k}}{\omega_{ck}} \tag{22}$$

and ω_{ck} is the cyclotron frequency in the emitter region. The relative width of the emitter strip is defined using the parameter ξ, where

$$\xi = \frac{\ell_k}{2r_{\perp k}} \tag{23}$$

and $\xi << 1 \Rightarrow$ narrow emitter

$\xi >> 1 \Rightarrow$ wide emitter

The perpendicular velocity of the electrons just above the cathode, $v_{\perp k}$, is given by,

$$v_{\perp k} = C \frac{E_{\perp k}}{H_k} \tag{24}$$

ii) Correlation of Gun and Cavity Parameters

Some parameters in the gun and cavity regions are correlated via the mirror ratio , α. It is assumed that the electron trajectories between the gun and cavity are adiabatic. Then,

$$R_k = \alpha^{1/2} R_e \tag{25}$$

$$v_{\perp} = \alpha^{1/2} v_{\perp k} \tag{26}$$

$$v_{\parallel} = \left(\frac{2e}{m} U - v_{\perp}^2\right)^{1/2} \tag{27}$$

iii) Velocity Spread

The velocity spread, $\Delta v_{\perp}/v_{\perp}$, must be held to a reasonably small value, of order 10%, in order to achieve high efficiency. An upper limit on the velocity spread is imposed by the condition that all electrons must have sufficient energy to pass through the high magnetic field region of the cavity. This implies,

$$g_o \equiv \sqrt{\frac{v_{\perp k}}{\Delta v_{\perp k}}} > \sqrt{\frac{\langle v_{\perp}^2 \rangle}{\langle v_{\parallel}^2 \rangle}} \tag{28}$$

Eq. (28) indicates that the velocity spread in the gun or injector (I) region limits the maximum ratio of average $v_{\perp}^2$ to $v_{\parallel}^2$ in the cavity region. Since a large value of $(v_{\perp}/v_{\parallel})$ is advantageous for energy extraction, a small $\Delta v_{\perp k}/v_{\perp k}$

is required. The degradation of gain in the cavity with increasing velocity spread is generally a more severe restriction than Eq. (28). Since the perpendicular velocity in the cavity, $v_\perp$ is approximately linearly related to $v_{\perp k}$ in the cathode region, according to

$$v_\perp = \alpha^{1/2} v_{\perp k} \quad ,$$

it follows that

$$\varepsilon \equiv \frac{\Delta v_\perp}{v_\perp} = \frac{\Delta v_{\perp k}}{v_{\perp k}} \tag{29}$$

so that velocity spread arising in the injector equals that in the cavity region. Velocity spread arises from several causes, including:

a) Space Charge at the Cathode

The velocity spread arising from space charge at the cathode is given approximately by:

$$\varepsilon_{sc} = \frac{\Delta v_\perp}{v_\perp} = \frac{I}{I_\rho} \tag{30}$$

where I_ρ (in statamps) must be separately evaluated in two limits: Narrow Emitter, $\xi << 1$. Then:

$$I_\rho = \frac{CR_k E_{\perp k}^2}{3B_k} \tag{31}$$

Wide Emitter, $\xi >> 1$. Then:

$$I_\rho = \frac{CR_k E_{\perp k}^2}{3B_k}\left(\frac{9}{4}\,\xi\phi_k\right)^{1/2} \tag{32}$$

For ϕ_k between 5 and 10 degrees, and $\xi \approx 5$, the quantity in parentheses in Eq. (32) is of order unity so that Eq. (31) and Eq. (32) are very nearly equal.

b) Thermal velocity of electrons.

The high temperature of the emitter strip, T_k, can lead to a velocity spread. Using $U_k = k_B T_k$,

$$\varepsilon_T = \frac{\Delta v_\perp}{v_\perp} = 3.6\left(1 + \frac{\pi^2}{4}\tan^2\phi_k\right)^{1/2}\left(\frac{U_k}{2r_{\perp k}E_k}\right)^{1/2} \tag{33}$$

c) Surface roughness of the cathode.

The major contribution to $\Delta v_\perp/v_\perp$ can be the surface roughness of the cathode. Assume the average height of the surface ripple to be a. Then,

$$\varepsilon_a = \frac{\Delta v_\perp}{v_\perp} = 1.4\left(1 + \frac{\pi^2}{4}\tan^2\phi_k\right)^{1/2}\left(\frac{a}{2r_{\perp k}}\right)^{1/2} \tag{34}$$

Using Eq. (27), and assuming U = const., we may show that

$$\left|\frac{dv_\parallel}{v_\parallel}\right| = \frac{\beta_\perp^2}{\beta_\parallel^2}\left|\frac{dv_\perp}{v_\perp}\right| = \beta_\perp^2\varepsilon/\beta_\parallel^2$$

D. Starting Current and Efficiency

i) Starting Current

The starting current, I_{st}, may be estimated for ω_c operation using:

$$I_{st}(A)(Q \times 10^{-3}) \frac{L}{\lambda} \frac{1}{\beta_{\parallel}^2} G e^{-2X^2} (\mu X - 1) = 2.3 \qquad (35)$$

where $I_{st}(A)$ is in amperes and

$$G = \frac{J_1^2(X_{op} R_e/R_o)}{X_{op}^2 J_o^2(X_{op})} \qquad (36)$$

$$X = \frac{1}{2}\left[\frac{1}{\mu} + \left(\frac{1}{\mu^2} + 1\right)^{1/2}\right] \qquad (37)$$

$$\mu = \pi \frac{\beta_{\perp}^2}{\beta_{\parallel}} \frac{L}{\lambda} \qquad (38)$$

The above expression assumes that the magnetic field is tuned to the resonance condition for the TE_{op1} mode. The effects of multimode operation on the starting current have been neglected. The EM fields in the cavity have been assumed to have a Gaussian distribution along z. We estimate that the starting current may be up to 2 to 4 times larger for a sinusoidal field variation.

It is also possible for a device designed to oscillate at ω_c to also oscillate at $2\omega_c$. The starting current may be estimated from an expression similar to Eq. (35), but is omitted here because the device efficiency will be very small if the device is designed for ω_c operation.

ii) Multimode Oscillation

A rough but simple estimate of mode competition may be made as follows. The peak gain for oscillation at ω occurs, using Eq.(14), at

$$\omega - k_{\parallel} v_{\parallel} = \omega_c$$

where $\omega = \frac{2\pi c}{\lambda} = \frac{2c}{D_o} X_{op}$

the gain bandwidth will not exceed $k_{\parallel}v_{\parallel}$ since the peak gain occurs at $\omega = \omega_c + k_{\parallel}v_{\parallel}$, but there is always absorption, rather than emission, when $\omega = \omega_c$. Hence, if mode TE_{op1} is set to oscillate, then a second mode, TE_{ab1} will not oscillate if

$$\left|\omega_{op} - \omega_{ab}\right| > 2k_{\parallel}v_{\parallel}$$

This may be rewritten

$$\frac{\left|X_{op} - X_{ab}\right|}{X_{op}} > \frac{\lambda}{L} \beta_{\parallel} \tag{39}$$

Here we are assuming a high Q cavity, $Q \gg \omega/k_{\parallel}v_{\parallel}$.

Eq. (39) is a rather stringent condition for preventing multimode oscillation, because the gain bandwidth is somewhat less than $k_{\parallel}v_{\parallel}$ and because there is a threshold for oscillation. Another cause of multimode oscillation is simultaneous excitation of a TE_{op1} and a TE_{op2} mode. These modes are separated by,

$$\frac{\omega_{op2} - \omega_{op1}}{\omega_{op1}} = \frac{3}{8} \frac{\lambda^2}{L^2} \tag{40}$$

The gain of the TE_{op2} mode is smaller than that of the TE_{op1} mode, so that the TE_{op2} mode is not expected to oscillate.

iii) Efficiency

The overall efficiency for conversion of beam power to output EM power is denoted η. Only the transverse energy of the electrons may be converted to output power. The transverse efficiency, $\eta_\perp$, may be estimated from the theory of Nusinovich and Erm. $\eta_\perp$ is a function of two parameters, μ, Eq. (38), and I_o, which, for ω_c operation, is given by:

$$I_o = 5.84\ I(A)(Q \times 10^{-3})\left(\frac{L}{\lambda}\right)^3\left(\frac{\beta_\perp}{\beta_\parallel}\right)^4 G \tag{41}$$

where G is defined by Eq. (36).

Given I_o and μ, $\eta_\perp$ is determined graphically using the theory of Nusinovich and Erm. In final gyrotron designs, the efficiency will be obtained from computer calculations of device saturated gain. Using $\eta_\perp$, the efficiency for conversion of electron beam power to internal cavity power, $\eta_{e\ell}$, is given by:

$$\eta_{e\ell} = \frac{\eta_\perp}{1 + (\beta_\parallel/\beta_\perp)^2} \tag{42}$$

When wall losses within the cavity are taken into account, the overall efficiency is,

$$\eta = \left[1 - \frac{Q}{Q_{OM}}\right]\eta_{e\ell} \tag{43}$$

where Q/Q_{OM} is derived from Eq. (10).

E. Design Considerations

In designing the gyrotron, a number of parameters must be specified. The specification of some parameters can lead to constraints on other parameters. Two crucial parameters which must be selected with great care are the cavity length (and shape) and the mirror ratio, α.

i. Cavity Length

The cavity shape and dimensions are of curcial importance in determining the cavity Q and the electron efficiency. Consequently, a final cavity design should rely on careful, computer calculations to optimize the efficiency.

A rough estimate of the cavity length may be obtained by the following argument. The optimum cavity length can be shown, for the gyrotrons of interest here, to be such that $L/\lambda >> 1$. The cavity dimensions, for a short wavelength device, will be very small. Such a small device will probably have a shape that does not deviate appreciably from a circular cylinder, such as the device shown in Fig. 1, because of the difficulty of fabricating more complex shapes of small dimensions. In that case,

$$Q_D = K\, 4\pi (L^2/\lambda^2)$$

with $K \approx 2$ to 4, Eq. 9. Although these K values seem reasonable, larger K values are possible. An additional constraint on L is obtained from the condition $Q_D << Q_{OM}$ in order to achieve high efficiency (Eq. 43). We may derive an upper limit on L by setting

$$Q_D \leq \frac{1}{4}\ Q_{OM} \tag{44}$$

so that $$\frac{L}{\lambda} \leq \left(\frac{\Lambda R_o/\delta}{16\pi K}\right)^{1/2} \tag{45}$$

In practice, the highest efficiency is often obtained by taking the highest possible value of L/λ, i.e. by setting L/λ equal to the right hand side of Eq. (45). The efficiency is calculated by using L/λ in Eqs. (38) and (41) and using the graphs of Nusinovich and Ern.

We should emphasize that these arguments yield a reasonable value of L/λ, but exact calculations appropriate for the actual cavity shape employed are required to truly optimize the efficiency. The use of an equality in Eq. (45) is not a strict rule and is not valid at long wavelengths or in harmonic operation.

ii) Mirror Ratio

Many parameters in the gun and cavity region are correlated by the mirror ratio , α. The selection of α is influenced by a number of constraints, as discussed below. First, it is important to indicate how a variety of paramenters scale with α.

a) Parameter Scaling with α.

The cavity parameters are assumed to be established, including λ, β_o, $\beta_\perp$ and R_e. These parameters, together with α, determine a number of gun parameters. For example,

$$
\begin{aligned}
B_k &= \alpha^{-1} B_o \\
R_k &= \alpha^{1/2} R_e \\
v_{\perp k} &= \alpha^{-1/2} \beta_\perp c \\
r_{\perp k} &= \frac{v_{\perp k}}{\omega_{ck}} \approx \frac{\alpha^{1/2} \beta_\perp \lambda}{2\pi} \\
E_{\perp k} &= \frac{v_{\perp k}}{c} B_k = \alpha^{-3/2} \beta_\perp B_o \\
I_\rho &= \alpha^{-3/2} \frac{c R_e \beta_\perp^2 B_o}{3} \quad , \text{ narrow emitter}
\end{aligned}
\tag{46}
$$

In addition, other gun parameters depend in part on α, such as:

$$\begin{aligned} \xi &= \ell_k/2r_{\perp k} \\ A &= 2\pi R_k \ell_k \\ h &= 2\pi^2 \phi_k\, r_{\perp k} \\ d &= V_1/E_{\perp k} \end{aligned} \tag{47}$$

where the α dependence may be obtained in each case from Eq. (46).

b) Constraints on the gun design.

1) Electric field strength in the cathode region

Electrical breakdown can occur between the cathode and first anode. If the maximum allowed $E_{\perp k}$ is $E_{\perp max}$, then

$$\begin{aligned} & E_{\perp max} \geq \alpha^{-3/2}\, \beta_{\perp} B_o \\ \text{or} \qquad & \alpha \geq (\beta_{\perp} B_o/E_{\perp max})^{2/3} \end{aligned} \tag{48}$$

2) Emitter current density.

Let the maximum allowed current density at the cathode emitter strip be J_{kmax}. Then, using Eq. (21),

$$J_{k\,max} \geq I/2\pi R_k \ell_k$$

If we assume that I is fixed, then

$$\alpha\xi \geq \frac{I}{2\beta_{\perp}\lambda R_e J_{k\,max}} \tag{49}$$

This yields a lower bound on the product $\alpha\xi$.

3) Velocity spread derived from space charge.

For a narrow emitter, letting

$$\varepsilon_{max} = (\Delta v_{\perp}/v_{\perp})max$$

and using Eqs. (30) and (31), we have

$$\left(\frac{\varepsilon_{max} c \; R_e \beta_{\perp}^2 B_o}{3I} \right)^{2/3} \geq \alpha \tag{50}$$

For a wide emitter,

$$\left(\frac{\varepsilon_{max} c \; R_e \beta_{\perp}^2 B_o}{3I} \right)^{2/3} \geq \alpha \left(\frac{9}{4} \; \xi \phi_k \right)^{-1/3} \tag{51}$$

4) Cathode to first anode spacing.

The condition $d > 2r_{\perp k}$ yeilds

$$\alpha > \frac{\beta_{\perp}^2 \lambda B_o}{\pi V_1} \tag{52}$$

5) Velocity spread derived from surface roughness.

Assuming $\pi^2 \tan^2 \phi_k << 4$, then, for a maximum ε_{max}, using Eq. (34),

$$\frac{\alpha}{a^2} \geq \frac{4\pi^2}{\varepsilon_{max}^4 \beta_{\perp}^2 \lambda^2} \tag{53}$$

A similar expression may be derived for the limit imposed by the velocity spread arising from the finite cathode temperature. That limit is generally less important than the one imposed by Eq. (53).

6) Conclusions concerning limits on α.

The preceding 5 subsections indicate that constraints are imposed on the value of α and other parameters. In fact, α will have both lower and upper bounds. Rather than attempt a comprehensive treatment of the selection of α and related parameters, we postpone such a discussion to the practical, numerical results derived below for a gyrotron of a specific frequency.

F. Wavelength Scaling of Gyrotron Parameters

As a check of the general formalism previously obtained, we compare some of the predictions of that theory with published Soviet theoretical and experimental results. In particular, we will compare with the results of Zaytsev et al. who have published the only data on high frequency gyrotrons.

i) General Wavelength Scaling

Zaytsev et al. have published a table listing a number of parameters and their scaling with wavelength, λ. The parameters that were assumed to be independent of wavelength were:

Electron beam voltage, U = constant

Electric field strength at the cathode, $E_{\perp k}$ = constant

$$\begin{aligned} R_o/\lambda &= \text{constant} \\ R_e/\lambda &= \text{constant} \\ \beta_\perp &= \text{constant} \\ \xi &= \text{constant} \end{aligned} \tag{54}$$

The constancy of $E_{\perp k}$ is probably related to high voltage breakdown. The invariance of R_o/λ and R_e/λ is related to maintaining the same cavity mode. Using Eq. (54) and previous equations we may derive the following results.

The skin depth, $\delta \sim \lambda^{1/2}$

Then $Q_{OM} \approx \dfrac{R_o}{\delta} \sim \dfrac{\lambda}{\lambda^{1/2}} = \lambda^{1/2}$

$$B_o \sim \omega_c \approx \omega \sim \lambda^{-1}$$

$$E_{\perp k} = \text{constant} = \alpha^{-3/2}\beta_\perp B_o$$

This yields, assuming $\beta_\perp$ = constant,

$$\alpha \sim \lambda^{-2/3}$$

Then
$$R_k = \alpha^{1/2} R_o \sim \lambda^{-1/3}\lambda = \lambda^{2/3}$$

$$r_{\perp k} = \alpha^{1/2} \beta_\perp \lambda / 2\pi \sim \lambda^{2/3}$$

$$\ell_k = \xi 2 r_{\perp k} \sim \lambda^{2/3}$$

$$B_k = \alpha^{-1} B_o \sim \lambda^{-1/3}$$

$$I_\rho = \alpha^{-3/2} \frac{C R_e \beta_\perp^2 B_o}{3} \sim \lambda$$

These results are listed in Table 1 and they are in agreement with the results of Zaytsev et al., although there are some additional values listed here. The wavelength scaling derived here depends strictly on the initial assumptions. These assumptions are not immutable, and it is possible, for example, to vary the cavity mode or energy, U, with wavelength. However, the derived scaling appears to represent the experience of the Soviet workers in high frequency gyrotrons.

Table 1. Wavelength Scaling

Parameter	λ dependence	Comment
U	constant	Assumption
$E_{\perp k}$	constant	Assumption
$\beta_{\perp}$, $\beta_{\parallel}$	constant	Assumption
ξ	constant	Assumption
R_o	λ	Assumption
R_e	λ	Assumption
δ	$\lambda^{1/2}$	
Q_{OM}	$\lambda^{1/2}$	
B_o	λ^{-1}	
α	$\lambda^{-2/3}$	
R_k	$\lambda^{2/3}$	
$r_{\perp k}$	$\lambda^{2/3}$	
ℓ_k	$\lambda^{2/3}$	
B_k	$\lambda^{-1/3}$	
I_ρ	λ	

ii) Efficiency vs. Wavelength

As an additional test of the present analysis, we have calculated, using the present theory, the efficiency of gyrotrons similar to those of Zaytsev et al. and have compared the calculated results with their experiments. The results are shown in Fig. 3. The assumed parameters were: U = 30 kV, I = 1 amp, $\beta_\perp/\beta_\parallel = 1.5$, a TE_{031} cavity mode, and $R_e/R_o = X_{12}/X_{03}$. The cavity was assumed to be a right circular cylinder, with diffractive Q, $Q_D = 3\ Q_{MIN}$. Calculations were carried out for ω_c and 2 ω_c operation. In each case, the ohmic Q was allowed to be R_o/δ, labelled "minimum losses" in Fig. 3, or 0.6 R_o/δ, labelled "realistic losses" in Fig. 3. At each wavelength, the cavity length, L, was varied in order to optimize the efficiency.

The present calculated efficiencies agree very well with those listed in the paper by Zaytsev et al. Although they used modes other than the TE_{031} in some cases, the variation of efficiency with cavity mode is not very important in low mode operation and is neglected here. The other parameters used here do agree with their experimental values.

In their paper, Zaytsev et al. stressed the good agreement obtained between their experimental and theoretical results. This agreement is evident in Fig. 3. The highest experimental point in Fig. 3 was obtained at ω_c, while the lower two experimental points, at short wavelength, were obtained at 2 ω_c.

The present theory, as shown in Fig. 3, indicates that the efficiency for ω_c operation decreases only slowly with wavelength until wavelengths less than 1 mm are reached. Operation at 2 ω_c is inherently inefficient for operation at short wavelengths.

G. References

1. A.V. Gaponov, A.L. Gol'denberg, D.P. Grigor'ev, T.B. Pankratova, M.I. Petelin and V.A. Flyagin, Radiophysics and Quantum Electron, 18, No.2, pp. 204-211, 1975 (English translation).
2. N.I. Zaytsev, T.B. Pankratova, M.I. Petelin and V.A. Flyagin, Radio Eng. Electron, Phys. 19, No.5 pp. 103-107, 1974 (in English).
3. D.V. Kisel', G.S. Kovablev, V.G. Navel'yev, M.I. Petelin and Sh. Ye. Tsimring, Radio Eng. Electron, Phys. 19, No. 4, pp. 95-100, 1974 (in English).
4. S.N. Vlasov, G.M. Zhislin, I.M. Orlova, M.I. Petelin and G.G. Rogacheva, Radiophysics and Quantum Electron., 12, No. 8, pp. 972-978, 1969 (in English).
5. A.L. Gol'denberg and M.I. Petelin, Radiophysics and Quantum Electron. 16, No. 1, pp. 106-111, 1973 (in English).
6. G.S. Nusinovich and R.E. Erm, Elektronnaya Tekhnika, Ser. 1, Elektronika SVCh, 1972, No. 2, 55.

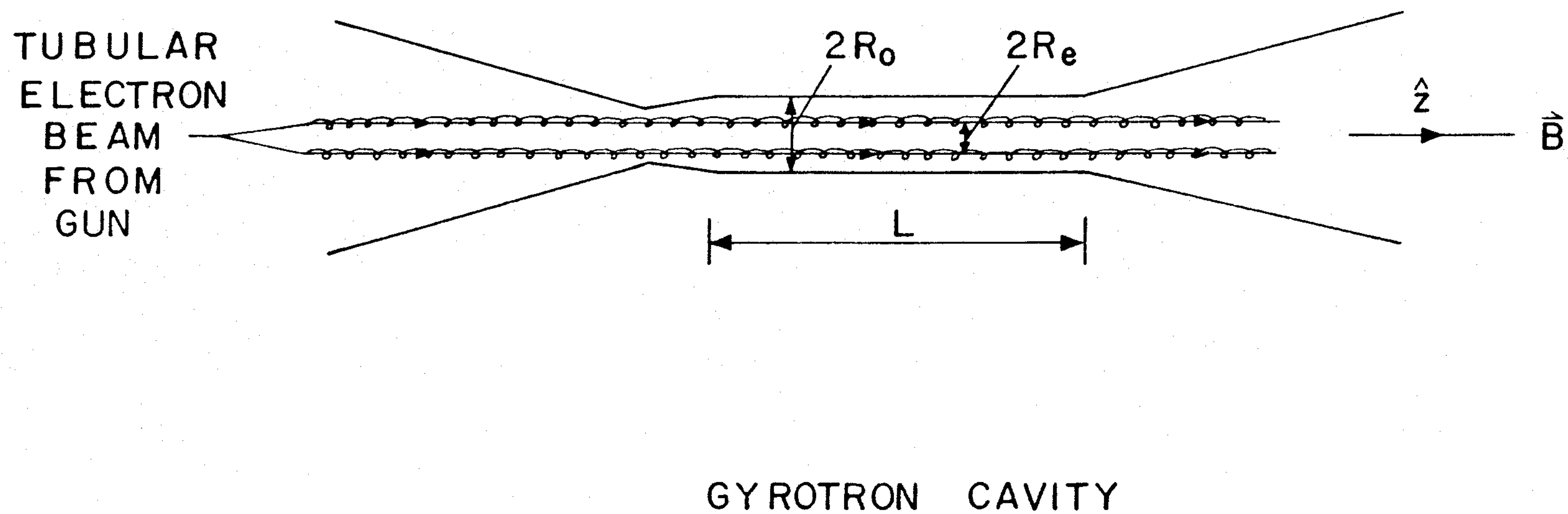

TUBULAR ELECTRON BEAM FROM GUN
$2R_o$
$2R_e$
L
$\hat{z}$
$\vec{B}$
GYROTRON CAVITY

Fig. I-1

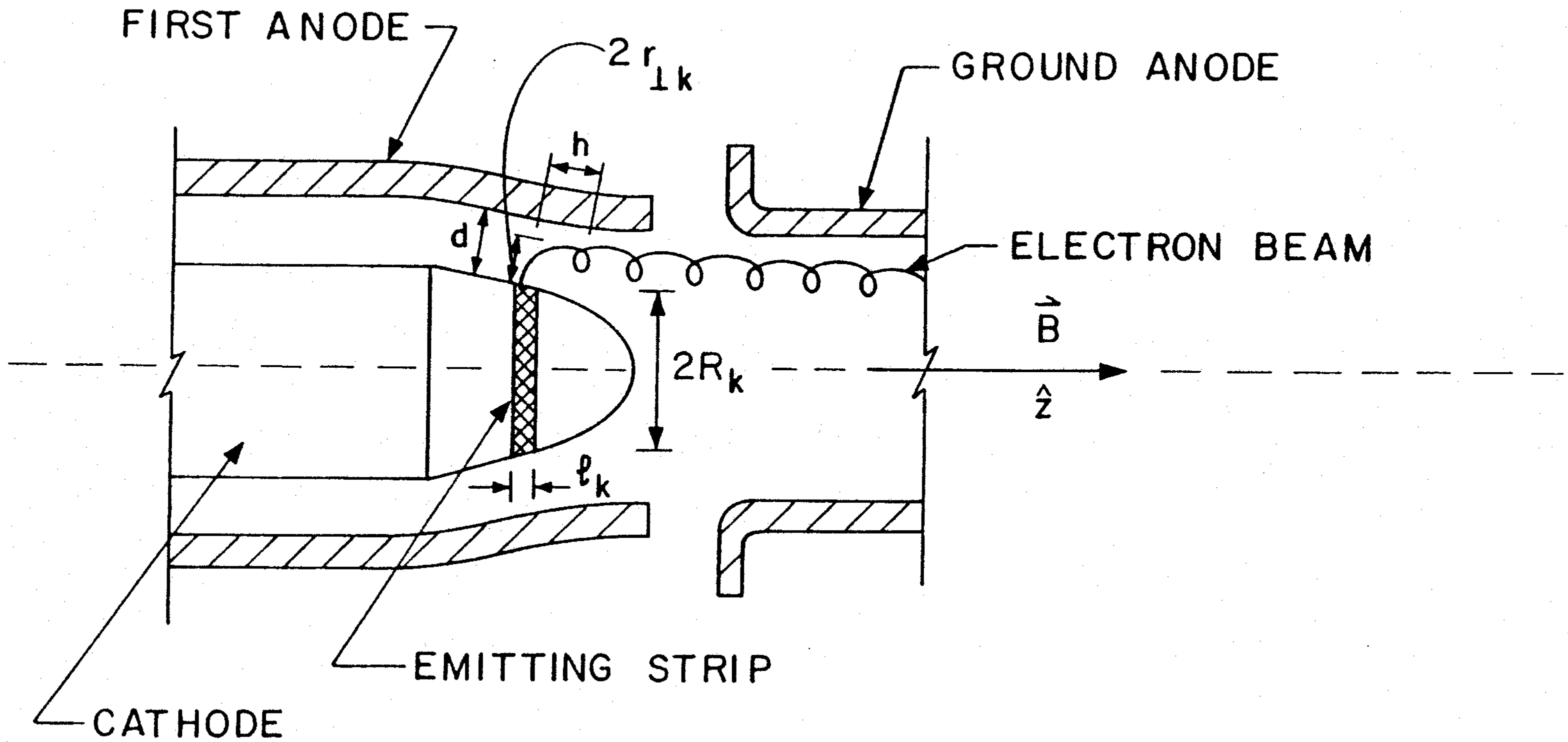

GYROTRON GUN

Fig. I-2

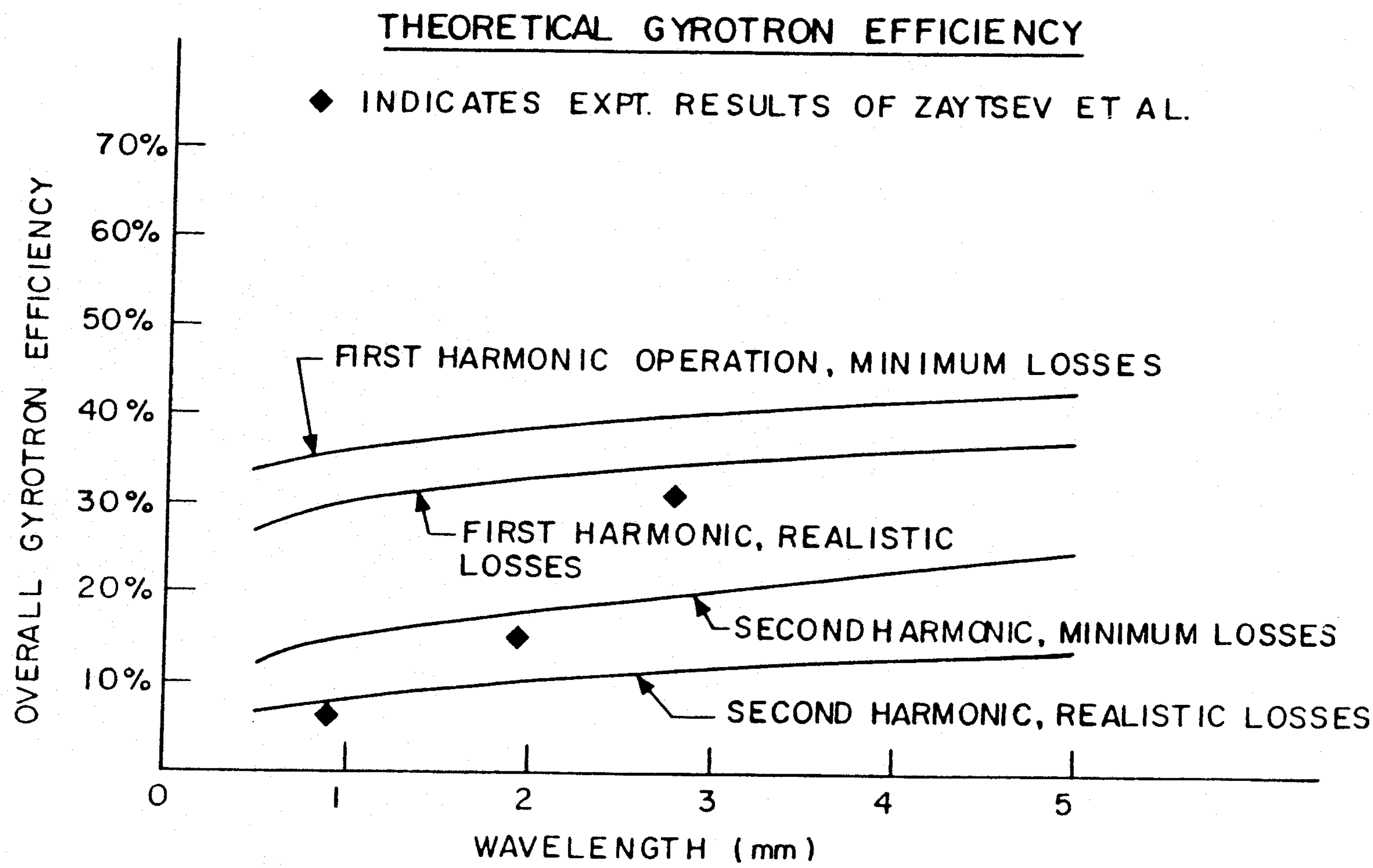

30 kV, 1 AMP BEAM, $\beta_\perp / \beta_{\parallel} = 1.5$, TE_{031} MODE
THEORY OF NUSINOVICH AND ERM

Fig. I-3

DESIGN STUDY FOR A

200 GHZ GYROTRON

Part II

R.J. TEMKIN, S.M. WOLFE

Francis Bitter National Magnet Laboratory
Massachusetts Institute of Technology
Cambridge, Massachusetts 02139 USA

March 9, 1978

GYROTRON DESIGN - 200 GHZ DEVICE

A. GYROTRON CAVITY

B. GYROTRON GUN

C. OUTPUT POWER

D. SCHEMATIC DRAWINGS

GYROTRON DESIGN - 200 GHZ DEVICE

In this section, we derive the operating parameters of a 200GHz gyrotron, $\lambda = 1.5$mm, working at $\omega \tilde{=} \omega_c$. The design is based on the general design principles described in a preceding section. The beam power is specified as 1 Amp at 30 kV, or 30 kW. With an efficiency of order 30%, an output power of about 10 kW is expected.

A. GYROTRON CAVITY

The cavity will be assumed to be similar in shape to Fig. 1. The working mode is taken to be a TE_{031} mode. $X_{03} = 10.173$. Assuming $L/\lambda >>1$, we have D_o = 4.86 mm and R_o = 2.43 mm. The electron beam is assumed to coincide with the second radial E field maximum, p=2. Then, since $X_{12} = 5.331$, R_e = 1.27 mm. Use of the second maximum allows the constriction at the cavity entrance to be small enough for cutoff of the RF field propagating out of the cavity toward the gun. The skin depth $\delta = 1.47 \times 10^{-5}$cm. $Q_{OM} = 1.65 \times 10^4 \Lambda$. For $\Lambda \approx 0.8$, $Q_{OM} = 1.32 \times 10^4$.

We determine the cavity length by setting $Q_D \approx \frac{1}{4} Q_{OM} = 4.13 \times 10^3$, as in Eq. (44), and assuming $Q_D \approx 3\, Q_{min}$, Eq. (9). Then $L/\lambda = 10.5$ and L = 15.8 mm. The value of $\omega/\omega_{cr} = 1.001$, which justifies using the large L/λ limit.

The value of γ is 1.0587 and β is 0.3284. Assume that $\beta_\perp/\beta_\parallel$ in the cavity region is 1.5. Then $\beta_\perp = 0.2732$, $\beta_\parallel = 0.1821$.

Using L, we obtain $k_\parallel = 1.99$ cm^{-1} and $k_\parallel v_\parallel = 1.086 \times 10^{10}$ sec^{-1}. Since $\omega = 1.257 \times 10^{12}$ sec^{-1}, $\omega_c = 1.246 \times 10^{12}$ sec^{-1} and B_o = 75.01 kG.

B. Gyrotron Gun

The gyrotron gun must produce a beam in the cavity region with the proper values of $\beta_\perp$ and $\beta_\parallel$ and with a minimal velocity spread. A key parameter in the gun design is the mirror ratio, α. As previously discussed, there are several constraints on the value of α. These may be summarized as follows:

$$E_{\perp\text{-max}} = 5 \times 10^4 \text{ V/cm} \longrightarrow \alpha \geq 25$$

$$J_{k\ max} = 3\text{A/cm}^2 \longrightarrow \alpha\xi \geq 32$$

$$\varepsilon_{max} = 0.1 \longrightarrow \begin{cases} 38 \geq \alpha & \text{(narrow emitter)} \\ 38 \geq \left(\frac{9}{4}\,\xi\phi_k\right)^{-1/3} & \text{(wide emitter)} \end{cases}$$

$$V_1 \gtrsim 5 \text{ kV};\ d > 2r_{\perp k} \longrightarrow \alpha > 16$$

$$\varepsilon_{max} = 0.1 \longrightarrow \alpha/a^2 \geq 2.35 \times 10^8 \text{ cm}^{-2}$$

In light of these constraints, we select the following gun parameters:

$$\alpha = 25$$

$$\xi = 1.3$$

$$a = 3\ \mu\text{m}$$

The value of ξ is such that the gun falls into neither the narrow nor the wide emitter regime. However, a rough value of ε can still be obtained from the narrow emitter equation since, as previously noted, a similar result for ε occurs for large and small ξ. This will be calculated below.

Using α and the scaling rules of Eq. (46), we obtain $B_k = 3.00$ kG, $R_k = 6.35$ mm, $\beta_{\perp k} = 0.05464$, $r_{\perp k} = 0.311$ mm, $E_{\perp k} = 1.64 \times 10^2$ statvolt/cm or $E_{\perp k} = 4.92 \times 10^4$ V/cm, $I_\rho = 5.69 \times 10^{10}$ statamps or $I_\rho = 19.0$A. The selected value of ξ yields the following parameters: $\ell_k = 0.81$ mm, A = 0.32 cm^2 and $J_k = 3.1$ A/cm^2. Let $V_1 \approx 8$ kV. Then d $\simeq$ 1.63 mm and $d/2\ r_{\perp k} = 2.6$,

$d/R_k = 0.26$. The gun angle ϕ_k is usually taken between 5 and 10^o. Assuming $\phi_k = 7.5^o$, $h = 0.80$ mm.

The velocity spread arises from several sources. The contribution from space charge at the cathode is $\varepsilon \simeq I/I_\rho$. I_ρ is estimated to be 19A using the narrow emitter approximation or 11.8 A using the wide emitter approximation. Hence $\varepsilon_{sc} \leq 8.5\%$ from space charge. The cathode temperature is assumed to be $T_k = 1200^oC$, $\varepsilon_T = 2.4\%$. Using $a = 3$ µm, $\varepsilon_a = 9.9\%$. The total $\varepsilon \simeq 13\%$.

C. Output Power

The starting current for the TE_{031} mode may now be estimated. Using $G = 1.89 \times 10^{-2}$ and $\mu = 13.5$, $I_{st} = 34$ mA. However, the actual I_{st} may be larger by a factor of 2-4.

The TE_{031} mode has a resonant frequency close to that of the TE_{231} mode. For the TE_{231} mode, $X_{23} = 9.969$. Then

$$\frac{X_{03} - X_{23}}{X_{03}} = 0.020 > 0.017 = \frac{\lambda}{L} \beta_{\parallel}$$

so that simultaneous oscillation of the TE_{231} and TE_{031} modes is unlikely.

The efficiency is obtained from the graphs of Nusinovich and Erm using $\mu = 13.5$ and $I_o = 2.0 \times 10^3$. The value found for $\eta_\perp$ is 0.6. Then $\eta_{e\ell} = 0.42$ and $\eta = 0.32$. The output power $P_{out} = \eta\, IU = 9.6$ kW.

D. Schematic Drawings

The 200 GHz gyrotron located in a Bitter magnet is illustrated schematically in the figure. Other figures illustrate the gyrotron gun and the gyrotron cavity.

200 GHz Gyrotron Parameters

$\upsilon = 200$ GHz	$B_o = 75.01$ kG	$\varepsilon = 13\%$
$\lambda = 1.5$ mm	$r_g = 0.0658$ mm	$G = 1.89 \times 10^{-2}$
$I = 1$ Amp	$\alpha = 25$	$\mu = 13.5$
$U = 30$ kV	$\xi = 1.3$	$Q = 3.15 \times 10^3$
TE_{031} mode	$a = 3$ μm	$I_{st} = 34$ mA
$X_{03} = 10.173$	$B_k = 3.00$ kG	$I_o = 2.0 \times 10^3$
$D_o = 2R_o = 4.86$ mm	$R_k = 6.35$ mm	$\eta_\perp = 0.60$
$R_e = 1.27$ mm	$\beta_{\perp k} = 0.05464$	$\eta_{e\ell} = 0.42$
$\delta = 1.47 \times 10^{-5}$cm	$\omega_{ck} = 5.28 \times 10^{10}$sec^{-1}	$\eta = 0.32$
$Q_{OM} = 1.32 \times 10^4$	$r_{\perp k} = 0.311$ mm	$P_{out} = 9.6$ kW
$Q_D = 4.13 \times 10^3$	$E_{\perp k} = 4.92 \times 10^4$V/cm	
$L/\lambda = 10.5$	$I_\rho = 19$ A	
$L = 15.8$ mm	$\ell_k = 0.81$ mm	
$\omega/\omega_{cr} = 1.001$	$A = 0.32$ cm^2	
$\gamma = 1.0587$	$J_k = 3.1$ A/cm^2	
$\beta = 0.3284$	$V_1 = 8$ kV	
$\beta_\perp/\beta_\parallel = 1.5$	$d = 1.63$ mm	
$\beta_\perp = 0.2732$	$\phi_k = 7.5^o$	
$\beta_\parallel = 0.1821$	$h = 0.80$ mm	
$k_\parallel = 1.99$ cm^{-1}	$T_k = 1200^o$C	
$k_\parallel v_\parallel = 1.086 \times 10^{10}$sec^{-1}	$\varepsilon_{sc} \lesssim 8.5\%$	
$\omega = 1.257 \times 10^{12}$sec^{-1}	$\varepsilon_T = 2.4\%$	
$\omega_c = 1.246 \times 10^{12}$sec^{-1}	$\varepsilon_a = 9.9\%$	

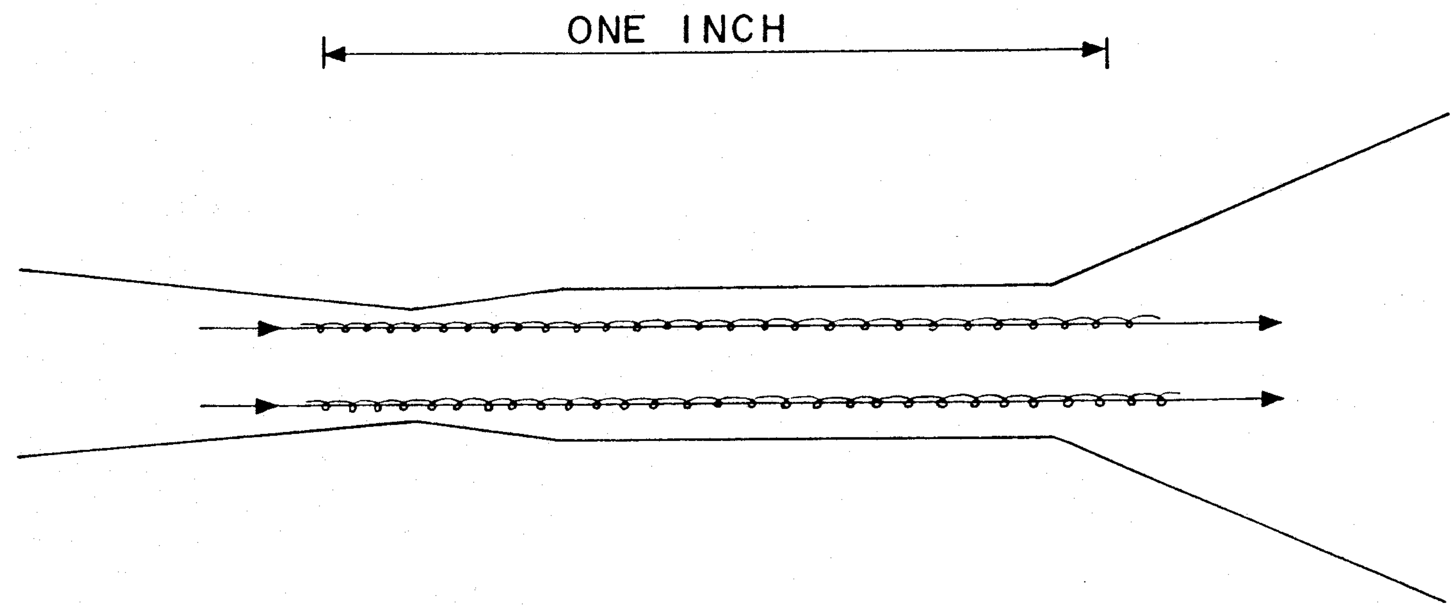

SCALE DRAWING OF TE_{031} CAVITY FOR
200 GHz GYROTRON

Fig. II-1

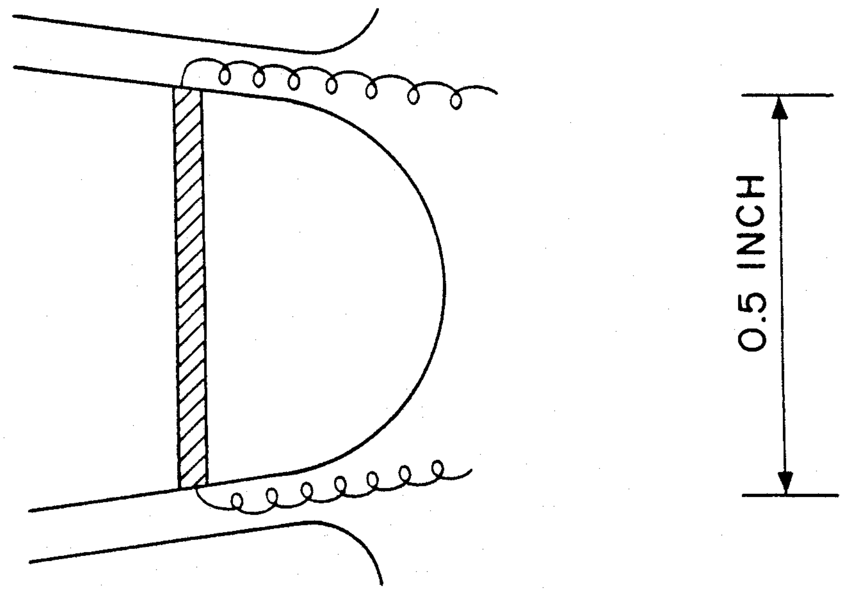

SCALE DRAWING OF ELECTRON GUN FOR
200 GHz GYROTRON

Fig. II-2

HIGH FREQUENCY GYROTRON USING BITTER MAGNET

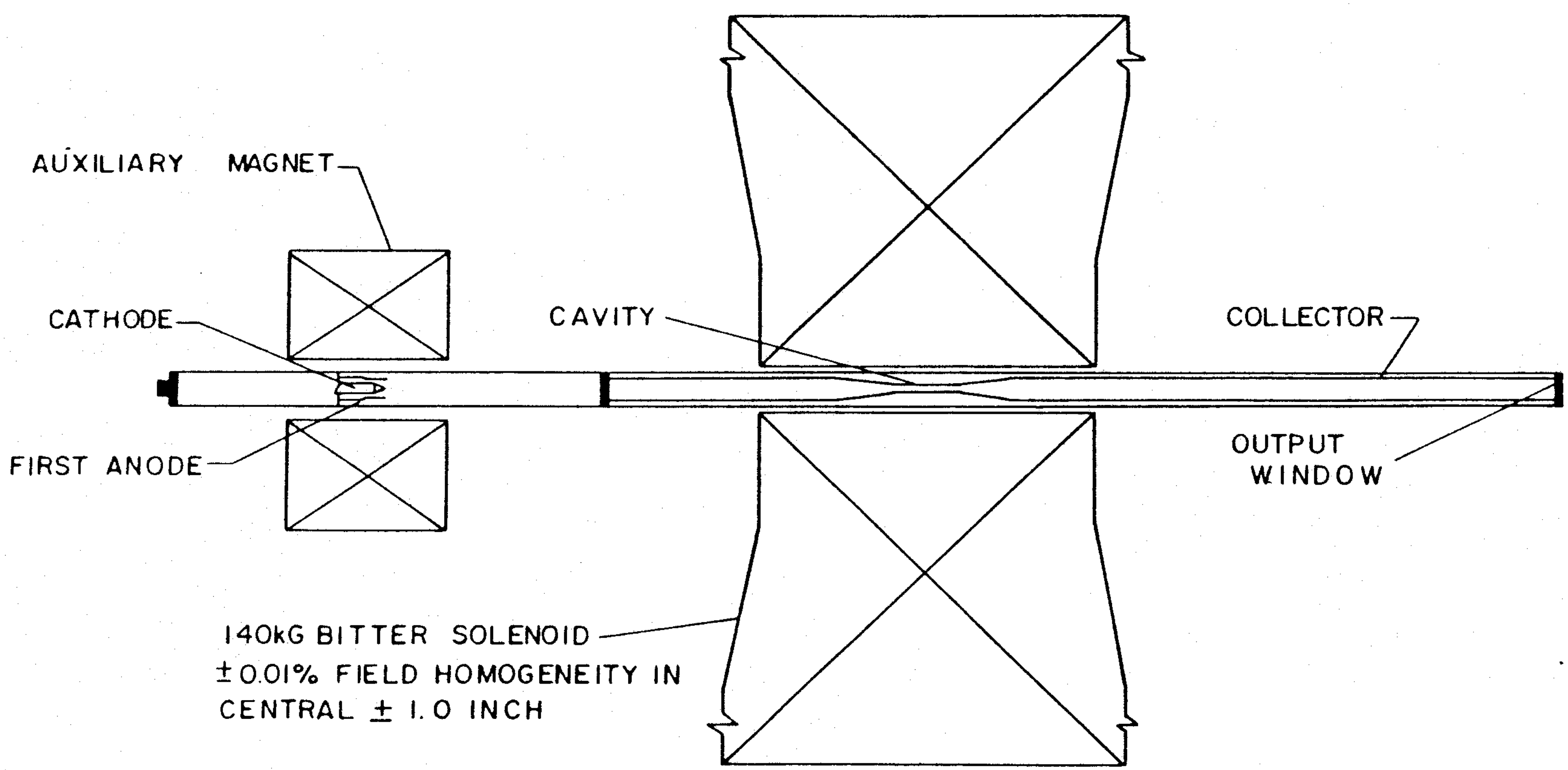

MAXIMUM OUTPUT FREQUENCY: 375 GHZ (0.80 mm), FIRST HARMONIC
750 GHZ (0.40 mm), SECOND HARMONIC

Fig. II-3